

Exotic mesons with double charm and bottom flavorS. Ohkoda,¹ Y. Yamaguchi,¹ S. Yasui,² K. Sudoh,³ and A. Hosaka¹¹*Research Center for Nuclear Physics (RCNP), Osaka University, Ibaraki, Osaka 567-0047, Japan*²*KEK Theory Center, Institute of Particle and Nuclear Studies, High Energy Accelerator Research Organization, 1-1, Oho, Ibaraki 305-0801, Japan*³*Nishogakusha University, 6-16, Sanbancho, Chiyoda, Tokyo 102-8336, Japan*

(Received 23 February 2012; published 21 August 2012)

We study exotic mesons with double charm and bottom flavor ($|C| = |B| = 2$), whose quark configuration is $\bar{Q}\bar{Q}qq$. This quark configuration has no annihilation process of quark and antiquark, and hence is a genuinely exotic state. We take a hadronic picture by considering the molecular states composed of a pair of heavy mesons, such as DD , DD^* , and D^*D^* for charm flavor, and BB , BB^* , and B^*B^* for bottom flavor. The interactions between heavy mesons are derived from the heavy quark effective theory. All molecular states are classified by $I(J^P)$ quantum numbers, and are systematically studied up to the total angular momentum $J \leq 2$. By solving the coupled channel Schrödinger equations, due to the strong tensor force of one-pion exchange, we find bound and/or resonant states of various quantum numbers.

DOI: [10.1103/PhysRevD.86.034019](https://doi.org/10.1103/PhysRevD.86.034019)

PACS numbers: 12.39.Jh, 12.39.Hg, 13.30.Eg, 14.20.-c

I. INTRODUCTION

Exotic hadrons which include multi-quark configurations provide us with important information in hadron physics. This is a key to understanding one of the most important problems in hadron physics: what are the constituent particles of hadrons, and what are the interactions among the constituent particles at relevant low energies? Those questions are related to the fundamental questions of the QCD, such as color confinement, chiral symmetry breaking, and so on. Nowadays the exotic hadrons are studied, not only in light flavor sectors, but also in heavy flavor sectors with charm and bottom quarks [1–5]. Recent experimental observations of heavy exotic hadrons, D_{sJ} , X , Y , Z^\pm in charm sector, and Y_b , Z_b^\pm in bottom sector have motivated intensive discussions about possible new dynamics in the heavy hadrons. Many of those hadrons have unusual mass, decay width, and branching ratios, which may not be explained as normal hadrons, such as $\bar{q}q$ and qqq . As candidates of flavor exotics for future experiments, a new hadron state T_{QQ} whose quark content is $\bar{Q}\bar{Q}qq$ has been discussed theoretically [6–35]. T_{QQ} is a system containing two heavy quarks and it is genuinely a flavor exotic which cannot be assigned by a normal hadron. In the present paper, we discuss the energy spectrum of the possible bound and/or resonant states of T_{QQ} .

In phenomenological studies, there exist two approaches to T_{QQ} state. In one approach, T_{QQ} is considered as a tetraquark state, in which the effective degrees of freedom are constituent quarks [6–31]. It is shown that T_{QQ} may be a stable object due to the strong attraction in qq which may form a stable scalar diquark [36–38]. As a result, T_{QQ} may be a deeply bound state, which does not decay through the strong interaction [22–24]. If the diquark developed, the study of T_{QQ} is also useful to understand the color superconductivity in high density quark matter [39–41]. The

tetraquark states such as T_{cc}^1 , T_{cb}^1 , and T_{bb}^1 states with $I(J^P) = 0(1^+)$ as well as T_{cb}^0 with $I(J^P) = 0(0^+)$ have been discussed also as stable objects [23,24].

Another approach is the hadronic molecule picture. When four quarks ($\bar{Q}\bar{Q}qq$) are present, they may form hadronic clusters ($\bar{Q}q$) which may alternatively become relevant degrees of freedom instead of diquarks [32–35]. The hadronic molecule picture is applied to the energy region close to the thresholds. In the T_{QQ} system, two mesons composed by $\bar{Q}q$, the pseudoscalar meson $P \sim (\bar{Q}q)_{\text{spin } 0}$ and the vector meson $P^* \sim (\bar{Q}q)_{\text{spin } 1}$, can become effective degrees of freedom as constituents. In the heavy quark limit, the pseudoscalar meson P and the vector meson P^* become degenerate in mass, and hence both of them should be considered. Hereafter we introduce the notation $P^{(*)}$ for P and P^* . Indeed, we will show that the mass degeneracy of the P and P^* activates the one-pion exchange potential between two $P^{(*)}$'s, and the bound and/or resonant $P^{(*)}P^{(*)}$ states are formed.

The tetraquark picture and the hadronic molecule picture are quite different. The tetraquark picture is applied to the deeply bound state. To apply this picture to the shallow bound states or resonant states, slightly below or above thresholds, respectively, is not appropriate, because the continuous $P^{(*)}$ states above thresholds are not taken into account. On the other hand, the hadronic molecule picture can be applied to the shallow and resonant states, while it cannot be applied to the deeply bound states.

Though there have been several studies for bound states of $P^{(*)}P^{(*)}$ in the hadronic molecule picture, resonant states of $P^{(*)}P^{(*)}$ have not been studied yet. Moreover, the quantum numbers $I(J^P)$ which have been discussed are limited only to $J \leq 1$. To be more problematic, several channels in the coupled channel problem have been neglected. The last point is very important in heavy quark systems. In the

heavy quark limit, we need to consider the mass degeneracy of P and P^* which provides more channels than discussed in the literature. In the present work, we discuss both bound and resonant states of $P^{(*)}P^{(*)}$ systematically for various quantum numbers $I(J^P)$ up to $J \leq 2$ by considering the fully coupled channel problem. The systematic analysis of the energy spectrum for various quantum numbers is important to investigate the dynamics governing the systems. Indeed, it will be shown that there are several new shallow bound and/or resonant states, which were not found in other studies, thanks to the strong attraction induced from the channel couplings even for larger J or angular momentum.

This paper is organized as follows. In Sec. II, we give the interaction between two $P^{(*)}$ meson based on the heavy quark symmetry and chiral symmetry. We introduce the two types of potentials: the π exchange potential and $\pi\rho\omega$ exchange potential. In Sec. III, we classify all the $P^{(*)}P^{(*)}$ systems up to $J = 2$, and search the bound and/or resonant states by applying the potentials and solving the Schrödinger equations numerically. In Sec. IV, we compare our results from the hadronic molecule picture with the previous results from the tetraquark picture. We summarize our discussions in the final section.

II. INTERACTION WITH TWO MESONS WITH DOUBLY HEAVY FLAVOR

The dynamics of the hadronic molecule of $P^{(*)}P^{(*)}$ respects two important symmetries; the heavy quark symmetry and chiral symmetry. The heavy quark symmetry induces the mass degeneracy of P and P^* in the heavy quark limit. Because of this, we have to consider the channels of degenerate pairs, such as PP , PP^* , P^*P , and P^*P^* , leading to the mixing of them: $PP^* - P^*P$, $P^*P^* - P^*P^*$, $PP - P^*P^*$, $PP^* - P^*P^*$.

As for the meson-exchange interaction between two $P^{(*)}$'s, the one-pion exchange potential (OPEP) exists at long distances. The existence of a pion is a robust consequence of spontaneous breaking of chiral symmetry [42]. The OPEP is provided by the $PP^*\pi$ and $P^*P^*\pi$ vertices whose coupling strengths are equally weighted thanks to the heavy quark symmetry. We note that there is no $PP\pi$ vertex because of the parity conservation. We should keep in mind in the following discussions that the existence of both $PP^*\pi$ and $P^*P^*\pi$ vertices—thanks to the heavy quark symmetry—provide the channel mixings in PP , PP^* , P^*P , and P^*P^* at long distance. We also introduce ρ and Ω meson-exchange to consider short range interaction.

To derive the $P^{(*)}P^{(*)}$ potential, we employ the effective Lagrangians based on the heavy quark symmetry and chiral symmetry [43–48]. They describe the interaction between heavy mesons which are given by the exchange of pion and vector mesons ($v = \rho, \omega$). The interaction Lagrangians are given as

$$\mathcal{L}_{\pi PP^*} = 2 \frac{g}{f_\pi} (P_a^\dagger P_{b\mu}^* + P_{a\mu}^{*\dagger} P_b) \partial^\mu \hat{\pi}_{ab}, \quad (1)$$

$$\mathcal{L}_{\pi P^* P^*} = 2i \frac{g}{f_\pi} \epsilon^{\alpha\beta\mu\nu} v_\alpha P_{a\beta}^{*\dagger} P_{b\mu}^* \partial_\nu \hat{\pi}_{ab}, \quad (2)$$

$$\mathcal{L}_{v PP} = -\sqrt{2} \beta g_V P_b P_a^\dagger v \cdot \hat{\rho}_{ba}, \quad (3)$$

$$\mathcal{L}_{v PP^*} = -2\sqrt{2} \lambda g_V v_\mu \epsilon^{\mu\nu\alpha\beta} (P_a^\dagger P_{b\beta}^* - P_{a\beta}^{*\dagger} P_b) \partial_\nu (\hat{\rho}_\alpha)_{ba}, \quad (4)$$

$$\mathcal{L}_{v P^* P^*} = \sqrt{2} \beta g_V P_b^* P_a^{*\dagger} v \cdot \hat{\rho}_{ba} + i2\sqrt{2} \lambda g_V P_{a\mu}^{*\dagger} P_{b\nu}^* (\partial^\mu (\hat{\rho}^\nu)_{ba} - \partial^\nu (\hat{\rho}^\mu)_{ba}), \quad (5)$$

where $P = D, B$, and $P_\mu^* = D_\mu^*, B_\mu^*$. The subscripts a and b are for light flavor indices, up and down, and v_μ is a four-velocity which will be fixed as $v_\mu = (1, \vec{0})$ below. The pion and vector meson (ρ and ω) fields are defined by

$$\hat{\pi} = \begin{pmatrix} \frac{\pi^0}{\sqrt{2}} & \pi^+ \\ \pi^- & -\frac{\pi^0}{\sqrt{2}} \end{pmatrix}, \quad \hat{\rho}_\mu = \begin{pmatrix} \frac{\rho^0 + \omega}{\sqrt{2}} & \rho^+ \\ \rho^- & -\frac{\rho^0 + \omega}{\sqrt{2}} \end{pmatrix}_\mu. \quad (6)$$

Following Ref. [48], the coupling constants in the interaction Lagrangians are given as

$$g = 0.59, \quad \beta = 0.9, \quad \lambda = 0.56 \text{ GeV}^{-1}, \quad (7)$$

$$f_\pi = 132 \text{ MeV}, \quad g_V = \frac{m_\rho}{f_\pi},$$

where f_π is the pion decay constant and m_ρ is the mass of the ρ meson. The OPEPs are derived by the interaction Lagrangians (1) and (2) as follows:

$$V_{P_1 P_2 \rightarrow P_1^* P_2^*}^\pi = \left(\sqrt{2} \frac{g}{f_\pi} \right)^2 \frac{1}{3} [\vec{\epsilon}_1^* \cdot \vec{\epsilon}_2 C(r; m_\pi) + S_{\epsilon_1^*, \epsilon_2} T(r; m_\pi)] \vec{\tau}_1 \cdot \vec{\tau}_2, \quad (8)$$

$$V_{P_1^* P_2^* \rightarrow P_1^* P_2^*}^\pi = \left(\sqrt{2} \frac{g}{f_\pi} \right)^2 \frac{1}{3} [\vec{T}_1 \cdot \vec{T}_2 C(r; m_\pi) + S_{T_1, T_2} T(r; m_\pi)] \vec{\tau}_1 \cdot \vec{\tau}_2, \quad (9)$$

$$V_{P_1 P_2 \rightarrow P_1^* P_2^*}^\pi = \left(\sqrt{2} \frac{g}{f_\pi} \right)^2 \frac{1}{3} [\vec{\epsilon}_1^* \cdot \vec{\epsilon}_2^* C(r; m_\pi) + S_{\epsilon_1^*, \epsilon_2^*} T(r; m_\pi)] \vec{\tau}_1 \cdot \vec{\tau}_2, \quad (10)$$

$$V_{P_1^* P_2^* \rightarrow P_1^* P_2^*}^\pi = -\left(\sqrt{2} \frac{g}{f_\pi} \right)^2 \frac{1}{3} [\vec{\epsilon}_1^* \cdot \vec{T}_2 C(r; m_\pi) + S_{\epsilon_1^*, T_2} T(r; m_\pi)] \vec{\tau}_1 \cdot \vec{\tau}_2, \quad (11)$$

where m_π is the pion mass. Here three polarizations are introduced for \mathbf{P}^* as defined by $\vec{\varepsilon}^{(\pm)} = (\mp 1/\sqrt{2}, -i/\sqrt{2}, 0)$ and $\vec{\varepsilon}^{(0)} = (0, 0, 1)$, and the spin-one operator \vec{T} is defined by $T_{\lambda'\lambda}^i = i\varepsilon^{ijk}\varepsilon_j^{(\lambda')\dagger}\varepsilon_k^{(\lambda)}$. As a convention, we assign $\vec{\varepsilon}^{(\lambda)}$ for an incoming vector particle and $\vec{\varepsilon}^{(\lambda)*}$ for an outgoing vector particle. Here $\vec{\tau}_1$ and $\vec{\tau}_2$ are isospin operators for $\mathbf{P}_1^{(*)}$ and $\mathbf{P}_2^{(*)}$; $\vec{\tau}_1 \cdot \vec{\tau}_2 = -3$ and 1 for the $I = 0$ and $I = 1$ channels, respectively. We define the tensor operators

$$S_{\varepsilon_1^*, \varepsilon_2} = 3(\vec{\varepsilon}^{(\lambda_1)*} \cdot \hat{r})(\vec{\varepsilon}^{(\lambda_2)} \cdot \hat{r}) - \vec{\varepsilon}^{(\lambda_1)*} \cdot \vec{\varepsilon}^{(\lambda_2)}, \quad (12)$$

$$S_{T_1, T_2} = 3(\vec{T}_1 \cdot \hat{r})(\vec{T}_2 \cdot \hat{r}) - \vec{T}_1 \cdot \vec{T}_2, \quad (13)$$

$$S_{\varepsilon_1^*, \varepsilon_2^*} = 3(\vec{\varepsilon}^{(\lambda_1)*} \cdot \hat{r})(\vec{\varepsilon}^{(\lambda_2)*} \cdot \hat{r}) - \vec{\varepsilon}^{(\lambda_1)*} \cdot \vec{\varepsilon}^{(\lambda_2)*}, \quad (14)$$

$$S_{\varepsilon_1^*, T_2} = 3(\vec{\varepsilon}^{(\lambda_1)*} \cdot \hat{r})(\vec{T}_2 \cdot \hat{r}) - \vec{\varepsilon}^{(\lambda_1)*} \cdot \vec{T}_2, \quad (15)$$

where $\hat{r} = \vec{r}/r$ is a unit vector between the two mesons.

The ρ meson exchange potentials are similarly obtained from the interaction Lagrangians (3)–(5),

$$V_{P_1 P_2 \rightarrow P_1 P_2}^\rho = \left(\frac{\beta g_V}{2m_\rho}\right)^2 \frac{1}{3} C(r; m_\rho) \vec{\tau}_1 \cdot \vec{\tau}_2, \quad (16)$$

$$V_{P_1 P_2^* \rightarrow P_1 P_2^*}^\rho = \left(\frac{\beta g_V}{2m_\rho}\right)^2 \frac{1}{3} C(r; m_\rho) \vec{\tau}_1 \cdot \vec{\tau}_2, \quad (17)$$

$$V_{P_1 P_2^* \rightarrow P_1^* P_2}^\rho = (2\lambda g_V)^2 \frac{1}{3} [2\vec{\varepsilon}_1^* \cdot \vec{\varepsilon}_2 C(r; m_\rho) - S_{\varepsilon_1^*, \varepsilon_2} T(r; m_\rho)] \vec{\tau}_1 \cdot \vec{\tau}_2, \quad (18)$$

$$V_{P_1^* P_2^* \rightarrow P_1^* P_2^*}^\rho = (2\lambda g_V)^2 \frac{1}{3} [2\vec{T}_1 \cdot \vec{T}_2 C(r; m_\rho) - S_{T_1, T_2} T(r; m_\rho)] \vec{\tau}_1 \cdot \vec{\tau}_2 + \left(\frac{\beta g_V}{2m_\rho}\right)^2 \frac{1}{3} C(r; m_\rho) \vec{\tau}_1 \cdot \vec{\tau}_2, \quad (19)$$

$$V_{P_1 P_2 \rightarrow P_1^* P_2^*}^\rho = (2\lambda g_V)^2 \frac{1}{3} [2\vec{\varepsilon}_1^* \cdot \vec{\varepsilon}_2^* C(r; m_\rho) - S_{\varepsilon_1^*, \varepsilon_2^*} T(r; m_\rho)] \vec{\tau}_1 \cdot \vec{\tau}_2, \quad (20)$$

$$V_{P_1 P_2^* \rightarrow P_1^* P_2^*}^\rho = -(2\lambda g_V)^2 \frac{1}{3} [2\vec{\varepsilon}_1^* \cdot \vec{T}_2 C(r; m_\rho) - S_{\varepsilon_1^*, T_2} T(r; m_\rho)] \vec{\tau}_1 \cdot \vec{\tau}_2. \quad (21)$$

The ω meson exchange potentials are obtained by replacing the mass of a ρ meson with that of a ω meson and by removing the isospin factor $\vec{\tau}_1 \cdot \vec{\tau}_2$. The OPEP's of $\mathbf{P}^{(*)}\mathbf{P}^{(*)}$ differ from the ones of $\mathbf{P}^{(*)}\bar{\mathbf{P}}^{(*)}$ in that the overall signs are changed due to G -parity. The situation is the same with ω meson exchange potentials, while ρ meson exchange

potentials of $\mathbf{P}^{(*)}\bar{\mathbf{P}}^{(*)}$ are not changed because the G -parity is even [49].

In the above equations, $C(r; m_h)$ and $T(r; m_h)$ are defined as

$$C(r; m_h) = \int \frac{d^3\vec{q}}{(2\pi)^3} \frac{m_h^2}{\vec{q}^2 + m_h^2} e^{i\vec{q}\cdot\vec{r}} F(\vec{q}; m_h), \quad (22)$$

$$T(r; m_h) S_{12}(\hat{r}) = \int \frac{d^3\vec{q}}{(2\pi)^3} \frac{-\vec{q}^2}{\vec{q}^2 + m_h^2} S_{12}(\hat{q}) e^{i\vec{q}\cdot\vec{r}} F(\vec{q}; m_h), \quad (23)$$

with $S_{12}(\hat{x}) = 3(\vec{\sigma}_1 \cdot \hat{x})(\vec{\sigma}_2 \cdot \hat{x}) - \vec{\sigma}_1 \cdot \vec{\sigma}_2$. We introduce the monopole type form factor at each vertex to take into account the size effect of $\mathbf{P}^{(*)}$ mesons. Its functional form is defined as

$$F(\vec{q}; m_h) = \left(\frac{\Lambda_P^2 - m_h^2}{\Lambda_P^2 + \vec{q}^2}\right)^2, \quad (24)$$

where m_h and \vec{q} are the mass and three-momentum of the exchanged meson h ($= \pi, \rho, \omega$) and Λ_P is the cutoff parameter. The cutoff parameters Λ_P are determined from the size of \mathbf{P} estimated from the constituent quark model, as discussed in Refs. [49–52]. The cutoff parameters are $\Lambda_D = 1121$ MeV and $\Lambda_B = 1070$ MeV when the π exchange potential is employed; they are $\Lambda_D = 1142$ MeV and $\Lambda_B = 1091$ MeV when the $\pi\rho\omega$ is employed.

Up to now we have given the meson-exchange potentials between two $\mathbf{P}^{(*)}$ mesons. We should note that the potentials contain spin operators and tensor operators; hence, the potentials for each quantum number are different. In the next section, we classify all the $\mathbf{P}^{(*)}\mathbf{P}^{(*)}$ states up to $J = 2$ and give the corresponding potentials in matrix form.

III. BOUND AND RESONANT STATES

Let us classify all the possible quantum numbers of the $\mathbf{P}^{(*)}\mathbf{P}^{(*)}$ systems with isospin I , total angular momentum J ($J \leq 2$), and parity P . We also need the principal quantum number $n = 0, 1, \dots$, if there exist several bound states for a given $I(J^P)$. We show the quantum numbers $I(J^P)$ and the channels in the wave functions in Table I. It is noted that the wave functions must be symmetric under the exchange of the two $\mathbf{P}^{(*)}$ mesons. We use the notation $^{2S+1}L_J$ to indicate the states with the internal spins S and angular momentum L . For example, the $I(J^P) = 0(1^+)$ state is a superposition of four channels; $\frac{1}{\sqrt{2}}(\mathbf{P}\mathbf{P}^* - \mathbf{P}^*\mathbf{P})(^3S_1)$, $\frac{1}{\sqrt{2}}(\mathbf{P}\mathbf{P}^* + \mathbf{P}^*\mathbf{P})(^3D_1)$, $\mathbf{P}^*\mathbf{P}^*(^3S_1)$, and $\mathbf{P}^*\mathbf{P}^*(^3D_1)$. All of the possible channels should be mixed for a given quantum number. In the previous studies, the channel mixings were not fully considered [33–35]. Here we pay attention to the approximate mass degeneracy of \mathbf{P} and \mathbf{P}^* , which plays a crucial role in mixing the channels. Otherwise, the attraction from the mixing effect becomes suppressed. We note that the tensor force is also important to mix the channels

TABLE I. Possible channels of $P^{(*)}P^{(*)}(2S+1L_J)$ for a set of quantum numbers I and J^P for $J \leq 2$.

| I | J^P | Components |
|-----|-------|---|
| | 0^- | $\frac{1}{\sqrt{2}}(PP^* + P^*P)(^3P_0)$ |
| | 1^+ | $\frac{1}{\sqrt{2}}(PP^* - P^*P)(^3S_1), \frac{1}{\sqrt{2}}(PP^* - P^*P)(^3D_1), P^*P^*(^3S_1), P^*P^*(^3D_1)$ |
| 0 | 1^- | $PP(^1P_1), \frac{1}{\sqrt{2}}(PP^* + P^*P)(^3P_1), P^*P^*(^1P_1), P^*P^*(^5P_1), P^*P^*(^5F_1)$ |
| | 2^+ | $\frac{1}{\sqrt{2}}(PP^* - P^*P)(^3D_2), P^*P^*(^3D_2)$ |
| | 2^- | $\frac{1}{\sqrt{2}}(PP^* + P^*P)(^3P_2), \frac{1}{\sqrt{2}}(PP^* + P^*P)(^3F_2), P^*P^*(^5P_2), P^*P^*(^5F_2)$ |
| | 0^+ | $PP(^1S_0), P^*P^*(^1S_0), P^*P^*(^5D_0)$ |
| | 0^- | $\frac{1}{\sqrt{2}}(PP^* - P^*P)(^3P_0), P^*P^*(^3P_0)$ |
| 1 | 1^+ | $\frac{1}{\sqrt{2}}(PP^* + P^*P)(^3S_1), \frac{1}{\sqrt{2}}(PP^* + P^*P)(^3D_1), P^*P^*(^5D_1)$ |
| | 1^- | $\frac{1}{\sqrt{2}}(PP^* - P^*P)(^3P_1), P^*P^*(^3P_1)$ |
| | 2^+ | $PP(^1D_2), \frac{1}{\sqrt{2}}(PP^* + P^*P)(^3D_2), P^*P^*(^1D_2), P^*P^*(^5S_2), P^*P^*(^5D_2), P^*P^*(^5G_2)$ |
| | 2^- | $\frac{1}{\sqrt{2}}(PP^* - P^*P)(^3P_2), \frac{1}{\sqrt{2}}(PP^* - P^*P)(^3F_2), P^*P^*(^3P_2), P^*P^*(^3F_2)$ |

with different angular momenta, L and $L \pm 2$. As a result, we obtain the Hamiltonian in a matrix form with the basis of those coupled channels. The explicit forms of the Hamiltonian for each $I(J^P)$ are summarized in the Appendix A.

Now we are ready to solve the coupled channel Schrödinger equations for each quantum number. The renormalized Numerov method [53] is adopted to numerically solve the coupled second-order differential equations. The resonant states are identified by the behavior of the phase shift δ as a function of the scattering energy E . The resonance position E_r is defined by an inflection point of the phase shift $\delta(E)$ and the resonance width by $\Gamma_r = 2/(d\delta/dE)_{E=E_r}$ following Refs. [49,51,54]. To check the consistency of our numerical calculations, we also adopt the complex scaling method, in which the resonant state is defined as a pole in the complex energy plane [54,55]. We obtain an agreement in the results of the renormalized Numerov method and the complex scaling method.

We summarize our numerical results for $D^{(*)}D^{(*)}$ bound/resonant states in Table II and Fig. 1. In $D^{(*)}D^{(*)}$ states, we find several bound and/or resonant states in $I = 0$, while there is no bound state in $I = 1$. In general, the attractive force of pion exchange in $I = 1$ is three times weaker than in $I = 0$ due to the isospin factor. As a numerical result, $D^{(*)}D^{(*)}$ bound states in $I = 1$ are not obtained but only resonant states are.

Let us look at our results one by one for each quantum number in detail. In the following text, most of the numerical values are those for the case of the $\pi\rho\omega$ potential, because the results from the $\pi\rho\omega$ potential are generally not so different from those from the π potential, except for the $0(2^-)$ state. The energies are measured from the threshold, which is defined to be the lowest mass among the channels for a given quantum number as tabulated in

Table I. For example, we adopt the DD^* mass as threshold for $I(J^P) = 0(0^-)$, while, the DD mass for $I(J^P) = 0(1^-)$.

- (i) $0(0^-)$ This state has only one channel of DD^* (see Table I) and the pion exchange potential is attractive as shown in Eq. (A14). As a result, the very deep bound state of DD^* is generated with binding energy 132.1 MeV measured from the DD^* threshold.

TABLE II. The energies of $D^{(*)}D^{(*)}$ states with $I(J^P)$ with $J \leq 2$. The energies E can be either pure real for bound states or complex for resonances. The real parts are measured from the thresholds as indicated in the third columns. The imaginary parts are half of the decay widths of the resonances, $\Gamma/2$. The values in the parentheses for the bound states are matter radii (relative distance of the two constituents) in units of fm.

| I | J^P | Threshold | E [MeV] | |
|-----|-------|-----------|---------------------------|-------------------------------|
| | | | π potential | π, ρ, ω potential |
| | 0^- | DD^* | -50.2(1.0) | -132.1(0.8) |
| | 1^+ | DD^* | -45.7(0.9) | -62.3(0.8) |
| 0 | 1^- | DD | $175.4 - i\frac{37.4}{2}$ | $152.8 - i\frac{10.6}{2}$ |
| | | | $19.4 - i\frac{63.0}{2}$ | $17.8 - i\frac{41.6}{2}$ |
| | 2^+ | DD^* | $34.5 - i\frac{183.1}{2}$ | $33.7 - i\frac{196.3}{2}$ |
| | 2^- | DD^* | $118.0 - i\frac{23.4}{2}$ | $112.1 - i\frac{26.6}{2}$ |
| | | | $0.1 - i\frac{0.02}{2}$ | -4.3(1.6) |
| | 0^+ | DD | no | no |
| | 0^- | DD^* | $143.8 - i\frac{40.0}{2}$ | $144.2 - i\frac{34.4}{2}$ |
| | | | $3.7 - i\frac{27.7}{2}$ | $2.3 - i\frac{37.4}{2}$ |
| 1 | 1^+ | DD^* | no | no |
| | 1^- | DD^* | no | no |
| | 2^+ | DD | $289.4 - i\frac{10.9}{2}$ | no |
| | 2^- | DD^* | no | no |

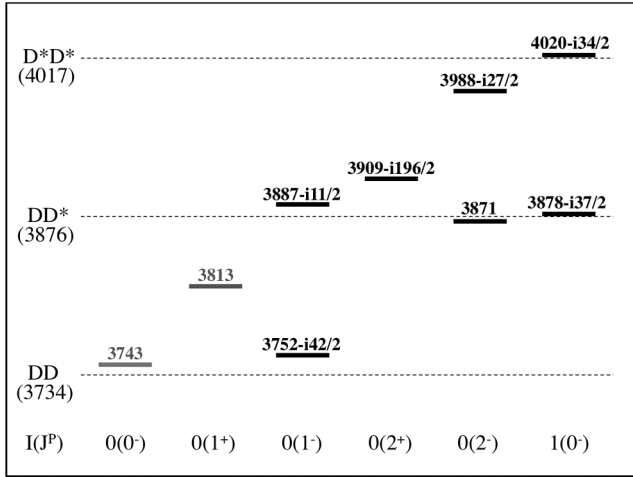


FIG. 1. Masses of $D^{(*)}D^{(*)}$ bound and resonant states for various $I(J^P)$. Solid lines are for our predictions with numerical values as denoted above the lines, and the values in parentheses below the lines denote the decay width Γ of the resonances when the $\pi\rho\omega$ potential is employed. Mass values are given in units of MeV. Compact objects which can not be regarded as molecular states are shown with gray lines.

- (ii) $0(1^+)$ The pion exchange potential is repulsive for diagonal components as shown in Eq. (A15). However, this state has four components and the mixing of the S and D waves causes the strong tensor attraction from the off-diagonal components of the potential. Consequently, there is a deeply bound state of mostly DD^* with binding energy 62.3 MeV measured from the DD^* threshold.
- (iii) $0(1^-)$ There are twin shape resonances of DD with the resonance energy 17.8 MeV and the decay width 41.6 MeV for the first resonance, and the resonance energy 152.8 MeV and the decay width 10.6 MeV for the second. The resonance energies are measured from the DD threshold. Those resonances are formed by the centrifugal barrier in the P wave.
- (iv) $0(2^+)$ This state contains only D wave components of DD^* and D^*D^* . The potential is weakly attractive. Nevertheless, due to the centrifugal barrier in the D wave, there is a shape resonance of DD^* scattering at the energy 33.7 MeV from the DD^* threshold, but the decay width 196.3 MeV is very wide.
- (v) $0(2^-)$ When the OPEP is employed, there are twin resonant states with the resonance energy 0.1 MeV and the decay width 0.02 MeV for the first resonance, and the resonance energy 118.0 MeV and the decay width 23.4 MeV for the second from the DD^* threshold. When the effects of ρ and ω meson exchange are included, the first resonance becomes a weakly bound state with the binding energy 4.3 MeV, because the ρ meson exchange enhances the central force attraction of the pion exchange. The ω meson exchange plays a minor role due to the

isospin factor, although this contribution suppresses the attractive central force. The second resonant state with the resonance energy 112.1 MeV and the decay width 26.6 MeV is not affected very much. From the analysis of wave function components of the two bound states, we have verified that the lower and higher states are dominated by DD^* and D^*D^* , respectively.

- (vi) $1(0^-)$ This is the only $I = 1$ state in $D^{(*)}D^{(*)}$. The interaction in $I = 1$ are either repulsive or only weakly attractive as already discussed. Nevertheless, due to the P wave centrifugal barrier, we find twin shape resonances; the resonance energy 2.3 MeV and the decay width 37.4 MeV for the first resonance, and the resonance energy 144.2 MeV and the decay width 34.4 MeV for the second, from the DD^* threshold.

Here several comments are in order. First, we have obtained several bound and/or resonant states even for $J = 2$. Here the long-range force by the OPEP becomes

TABLE III. The energies of $B^{(*)}B^{(*)}$ states with $I(J^P)$ with $J \leq 2$. (Same convention as Table II).

| I | J^P | Threshold | $E - i\Gamma/2$ [MeV] | | |
|-------|--------|--------------------------|--------------------------|-------------------------------|-----------|
| | | | π potential | π, ρ, ω potential | |
| 0 | 0^- | BB^* | -32.0(1.2) | -77.5(0.9) | |
| | | | -178.0(0.6) | -305.9(0.5) | |
| | 1^+ | BB^* | -25.7(1.2) | -33.6(1.1) | |
| | | | -179.7(0.5) | -201.5(0.5) | |
| | 1^- | BB | $52.8 - i\frac{12.8}{2}$ | $35.0 - i\frac{11.8}{2}$ | |
| | | | $1.9 - i\frac{3.3}{2}$ | -3.1(1.6) | |
| | | | -39.1(0.8) | -98.9(0.6) | |
| | | | -125.5(0.6) | -164.4(0.5) | |
| | | | $5.5 - i\frac{5.9}{2}$ | $5.7 - i\frac{13.2}{2}$ | |
| | | | -51.2(0.8) | -60.6(0.8) | |
| 2^+ | BB^* | $26.9 - i\frac{20.2}{2}$ | $7.6 - i\frac{4.3}{2}$ | | |
| | | $7.6 - i\frac{4.3}{2}$ | $0.5 - i\frac{8.5}{2}$ | | |
| | | -68.7(0.8) | -84.1(0.7) | | |
| | | -147.5(0.6) | -196.5(0.6) | | |
| 1 | 0^+ | BB | -18.1(0.9), | -33.9(0.5) | |
| | 0^- | BB^* | $46.7 - i\frac{1.9}{2}$ | | |
| | | | $0.7 - i\frac{3.0}{2}$ | $38.5 - i\frac{4.6}{2}$ | |
| | | | | -50.5(0.8) | -5.9(1.4) |
| | 1^+ | BB^* | -38.1(0.8) | no | |
| | 1^- | BB^* | no | $11.7 - i\frac{11.0}{2}$ | |
| | 2^+ | BB | $23.0 - i\frac{4.4}{2}$ | $62.4 - i\frac{52.5}{2}$ | |
| | 2^- | BB^* | $63.7 - i\frac{7.6}{2}$ | | |
| | | | $2.0 - i\frac{3.3}{2}$ | $2.3 - i\frac{4.7}{2}$ | |

effective for the extended objects with large angular momenta. It is also interesting to have “twin states” for several quantum numbers, $0(1^-)$, $0(2^-)$, and $1(0^-)$. We have to note that the channel couplings by D and D^* are important to produce the obtained energy spectrum. Indeed, if we cut the channel coupling, we confirm that many of the states disappear. Thus, we consider that the pattern of the energy spectrum is reflected by the dynamics of the fully coupled channels.

Second, the present formalism of the hadronic molecule picture cannot be applied to compact objects. When the two $P^{(*)}$ mesons overlap spatially, we need to consider the internal structure of $P^{(*)}$, which is not included in the present hadronic picture. Therefore we shall adopt 1 fm or larger for the size of the bound state to be interpreted as a molecular state. The size of 1 fm is twice that of a typical radius of $P^{(*)} \sim 0.5$ fm. For instance, the $I(J^P) = 0(2^-)$ bound state with the binding energy -4.3 MeV is identified with a molecular state because it has the size 1.6 fm, while the $I(J^P) = 0(0^-)$ bound state with -132.1 MeV is not because its size is 0.8 fm. We emphasize, however, that this criterion is not definitive but gives only a qualitative guide.

Next we discuss the $B^{(*)}B^{(*)}$ states. We use the same coupling constants, and change only the masses of heavy mesons with small differences in the cutoff parameters. The results are summarized in Table III and Figs. 2 and 3. At first glance, we find that the $B^{(*)}B^{(*)}$ states have many bound and resonant states in comparison with the $D^{(*)}D^{(*)}$ states. There are two reasons. First, the kinetic term is suppressed in the Hamiltonian because the reduced mass becomes larger in the bottom sector. Second, the effect of channel couplings becomes more important, because a pseudoscalar meson B and a vector meson B^* become

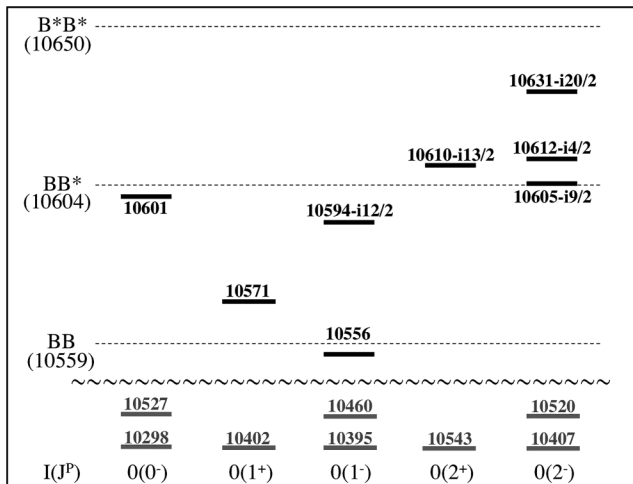


FIG. 2. The $B^{(*)}B^{(*)}$ bound and resonant states around the thresholds with $I(J^P)$ in $I = 0$. Compact objects which cannot be regarded as molecular states are shown below the wavy line, but their locations do not reflect the correct energy scale. (Same convention as Fig. 1.)

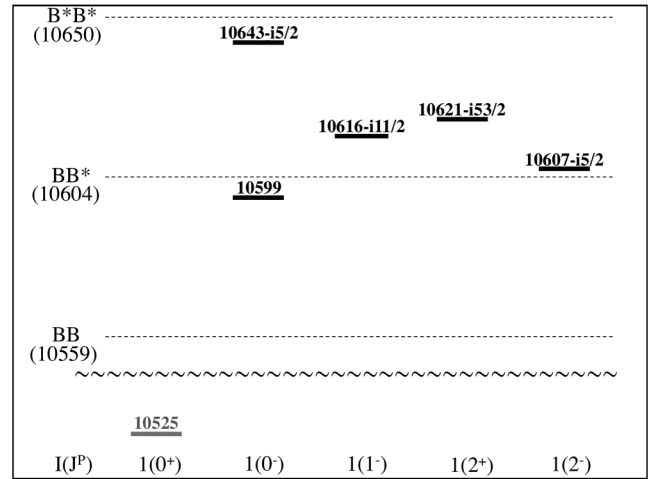


FIG. 3. The $B^{(*)}B^{(*)}$ bound and resonant states around the thresholds with $I(J^P)$ in $I = 1$. (Same convention as Fig. 1.)

more degenerate thanks to the heavy quark symmetry; similar discussion has been done in Refs. [49–51]. We note that, as a consequence of the strong attraction, several new states appear in the $B^{(*)}B^{(*)}$ states in isospin triplet: $I(J^P) = 1(0^+)$, $1(1^-)$, $1(2^+)$, and $1(2^-)$. The corresponding states are not obtained in the $D^{(*)}D^{(*)}$ states.

As noted in the charm sector, the deeply bound states will not be within the scope of the hadronic molecule picture. In the bottom sector, due to more attraction, more bound states are generated. For example, we have three states ($n = 0, 1, 2$) in the $0(0^-)$ state. However, the $n = 0, 1$ states are too compact (0.5 and 0.9 fm, respectively) to be considered as hadronic molecules. The $n = 2$ state is an extended object (2.5 fm), and hence can be considered as a hadronic molecule. Similarly, it would not be conclusive yet to consider hadronic molecules for the following states with radii less than 1 fm: the $n = 0$ state in $0(1^+)$; the $n = 0, 1$ states in $0(1^-)$; the $n = 0$ state in $0(2^+)$; the $n = 0, 1$ states in $0(2^-)$; and the $n = 0$ state in $1(0^+)$.

IV. HADRONIC MOLECULES AND TETRAQUARKS

In the present paper, we have considered T_{QQ} as a hadronic molecule composed by $P^{(*)}P^{(*)}$ in which one-pion exchange potential induces a dominant attraction. On the other hand, as mentioned in the introduction, T_{QQ} can also be considered as a tetraquark $\bar{Q}Qqq$ in which a diquark qq provides a strong binding energy. The different features between the hadronic molecule and tetraquark pictures are seen in their sizes. For hadronic molecules to be valid, hadron constituents must be sufficiently far apart such that their identities as hadrons are maintained. They cannot be close enough to overlap one another. Therefore, masses of hadronic molecules should appear around their threshold regions. In contrast, tetraquarks may be strongly bound and become compact objects as genuine quark

objects. Thus, their natures are distinguished by their energies, whether they have a small binding energy of order 10 MeV or less, or they have a larger binding energy.. Although it is tempting to seek for a framework to cover both scales, such a problem is beyond the scope of the present paper. Instead, we compare the results from the two pictures and just clarify the differences between them.

In the hadronic molecule picture by $P^{(*)}P^{(*)}$, as presented in the previous section, we obtain not only the bound states, but also the resonant states in many $I(J^P)$ quantum numbers. Both in charm and bottom sectors, it is remarkable that there are even the twin states in several quantum numbers, $0(1^-)$, $0(2^-)$, and $1(0^-)$.

In the tetraquark picture including a diquark model [23,24,27,29], in contrast, only two bound states in $I(J^P) = 0(1^+)$ and $1(2^-)$ have been predicted until now, as discussed for example in Refs. [27–29] as recent works. For $0(1^+)$, the predicted binding energy can be around 70 MeV from the DD^* threshold. For $1(2^-)$, the predicted binding energy can be around 27 MeV. The mass of the $0(1^+)$ states in the tetraquark picture is accidentally close to our value 62 MeV in the hadronic molecule picture. However, this comparison should be considered more carefully. Because the size of the $0(1^+)$ state is 0.8 fm from Table II, the D and D^* mesons composing the $0(1^+)$ state would be overlapped spatially if the size of each D and D^* meson has a scale of about 1 fm. In such a compact object, the quark degrees of freedom may become active to contribute to the dynamics like the tetraquark picture. However, such an effect is beyond the scope of the present hadronic molecule picture. The $1(2^-)$ state cannot be found in our present study.

In any cases, the feature in the energy spectrum in the $D^{(*)}D^{(*)}$ molecule picture is that there are many shallow bound states and resonances in $0(1^-)$, $0(2^+)$, $0(2^-)$, and $1(0^-)$, which are not found in the tetraquark picture. Thus, we observe that the energy spectrum of the hadronic molecule picture by $P^{(*)}P^{(*)}$ is qualitatively different from that of the tetraquark picture.

V. SUMMARY

We have discussed exotic mesons with double charm and bottom flavor whose quark content $\bar{Q}\bar{Q}qq$ is genuinely exotic. We have taken the hadronic picture, and considered molecular states of two heavy mesons $P^{(*)}$'s (a pseudoscalar meson $P = D, B$, and a vector meson $P^* = D^*, B^*$). By respecting heavy quark and chiral symmetries, we have constructed the π exchange potential and the $\pi\rho\omega$ exchange potential between the two heavy mesons. To investigate the bound and/or resonant states, we have numerically solved the coupled channel Schrödinger equations for the $P^{(*)}P^{(*)}$ states with $I(J^P)$ for $J \leq 2$.

As results, we have found many bound and/or resonant states in both charm and bottom sectors. The $D^{(*)}D^{(*)}$ bound and resonant states have moderate energies and

decay widths around the thresholds in several channels with quantum numbers: $0(0^-)$, $0(1^+)$, $0(1^-)$, $0(2^+)$, $0(2^-)$, and $1(0^-)$. The $B^{(*)}B^{(*)}$ states have more bound and resonant states with various quantum numbers. Several new states appear in the $B^{(*)}B^{(*)}$ states in isotriplet states, such as $1(0^+)$, $1(1^-)$, $1(2^+)$, and $1(2^-)$, which cannot be found in the charm sector. By contrast to the $D^{(*)}D^{(*)}$ states, some $B^{(*)}B^{(*)}$ states are very compact objects with a large binding energy much below the thresholds. Perhaps these states cannot survive as hadronic molecules and more consideration of quark dynamics such as tetraquarks is required.

The energy spectrum for quantum numbers $I(J^P)$ will help us to study the structure of the exotic states with $\bar{Q}\bar{Q}qq$. In the present hadronic molecule picture, many shallow bound states and resonant states appear around the thresholds in several quantum numbers. Indeed, they were not found in the tetraquark picture. It is interesting to note that, around the thresholds for $0(1^-)$, $0(2^+)$, $0(2^-)$, and $1(0^-)$, the shape of the energy spectrum in those states in the charm sector looks similar to that in the corresponding states in the bottom sector. It may indicate a universal behavior of the energy spectrum around the thresholds.

Experimental studies of those exotic hadrons should be performed in the near future. The double charm production in accelerator facilities will help us to search them [56]. Recently, it has been discussed that the quark-gluon plasma in the relativistic heavy ion collisions could produce an abundance of exotic hadrons, including the exotic mesons with double charm [57,58]. Those experimental studies will shed light on the nature of the exotic mesons with double charm and bottom flavor, and provide important hints to the fundamental questions of the strong interaction in hadron physics.

ACKNOWLEDGMENTS

We thank Professor S. Takeuchi and Professor M. Takizawa for fruitful discussions and comments. This work is supported in part by Grant-in-Aid for Scientific Research on Priority Areas ‘‘Elucidation of New Hadrons with a Variety of Flavors (E01: 21105006)’’ (S. Y. and A. H.) and by ‘‘Grant-in-Aid for Young Scientists (B) 22740174’’ (K. S.), from the ministry of Education, Culture, Sports, Science and Technology of Japan.

APPENDIX: HAMILTONIAN

The Hamiltonian is a sum of the kinetic term and potential term as

$$H_{I(J^P)} = K_{I(J^P)} + V_{I(J^P)}^\pi \quad (\text{A1})$$

for the π exchange potential only, and

$$H_{I(J^P)} = K_{I(J^P)} + \sum_{i=\pi,\rho,\omega} V_{I(J^P)}^i \quad (\text{A2})$$

for the $\pi\rho\omega$ potential.

The kinetic terms, including the explicit breaking of the heavy quark symmetry by the mass difference $\Delta m_{PP^*} = m_{P^*} - m_P$, are

$$K_{0(0^-)} = \text{diag}\left(-\frac{1}{2\tilde{m}_{PP^*}} \Delta_1\right), \quad (\text{A3})$$

$$K_{0(1^+)} = \text{diag}\left(-\frac{1}{2\tilde{m}_{PP^*}} \Delta_0, -\frac{1}{2\tilde{m}_{PP^*}} \Delta_2, -\frac{1}{2\tilde{m}_{P^*P^*}} \Delta_0 + \Delta m_{PP^*}, -\frac{1}{2\tilde{m}_{P^*P^*}} \Delta_2 + \Delta m_{PP^*}\right), \quad (\text{A4})$$

$$K_{0(1^-)} = \text{diag}\left(-\frac{1}{2\tilde{m}_{PP}} \Delta_0, -\frac{1}{2\tilde{m}_{PP}} \Delta_1 + \Delta m_{PP^*}, -\frac{1}{2\tilde{m}_{P^*P^*}} \Delta_1 + 2\Delta m_{PP^*}, -\frac{1}{2\tilde{m}_{P^*P^*}} \Delta_1 + 2\Delta m_{PP^*}, -\frac{1}{2\tilde{m}_{P^*P^*}} \Delta_3 + 2\Delta m_{PP^*}\right), \quad (\text{A5})$$

$$K_{0(2^+)} = \text{diag}\left(-\frac{1}{2\tilde{m}_{PP^*}} \Delta_2, -\frac{1}{2\tilde{m}_{P^*P^*}} \Delta_2 + \Delta m_{PP^*}\right), \quad (\text{A6})$$

$$K_{0(2^-)} = \text{diag}\left(-\frac{1}{2\tilde{m}_{PP^*}} \Delta_1, -\frac{1}{2\tilde{m}_{PP^*}} \Delta_3, -\frac{1}{2\tilde{m}_{P^*P^*}} \Delta_1 + \Delta m_{PP^*}, -\frac{1}{2\tilde{m}_{P^*P^*}} \Delta_3 + \Delta m_{PP^*}\right), \quad (\text{A7})$$

$$K_{1(0^+)} = \text{diag}\left(-\frac{1}{2\tilde{m}_{PP}} \Delta_0, -\frac{1}{2\tilde{m}_{PP}} \Delta_0 + 2\Delta m_{PP^*}, -\frac{1}{2\tilde{m}_{PP^*}} \Delta_2 + 2\Delta m_{PP^*}\right), \quad (\text{A8})$$

$$K_{1(0^-)} = \text{diag}\left(-\frac{1}{2\tilde{m}_{PP^*}} \Delta_1, -\frac{1}{2\tilde{m}_{P^*P^*}} \Delta_1 + \Delta m_{PP^*}\right), \quad (\text{A9})$$

$$K_{1(1^+)} = \text{diag}\left(-\frac{1}{2\tilde{m}_{PP^*}} \Delta_0, -\frac{1}{2\tilde{m}_{PP^*}} \Delta_2, -\frac{1}{2\tilde{m}_{P^*P^*}} \Delta_2 + \Delta m_{PP^*}\right), \quad (\text{A10})$$

$$K_{1(1^-)} = \text{diag}\left(-\frac{1}{2\tilde{m}_{PP^*}} \Delta_1, -\frac{1}{2\tilde{m}_{P^*P^*}} \Delta_1 + \Delta m_{PP^*}\right), \quad (\text{A11})$$

$$K_{1(2^+)} = \text{diag}\left(-\frac{1}{2\tilde{m}_{PP}} \Delta_2, -\frac{1}{2\tilde{m}_{PP}} \Delta_2 + \Delta m_{PP^*}, -\frac{1}{2\tilde{m}_{P^*P^*}} \Delta_2 + 2\Delta m_{PP^*} - \frac{1}{2\tilde{m}_{P^*P^*}} \Delta_0 + 2\Delta m_{PP^*}, -\frac{1}{2\tilde{m}_{P^*P^*}} \Delta_2 + 2\Delta m_{PP^*}, -\frac{1}{2\tilde{m}_{P^*P^*}} \Delta_4 + 2\Delta m_{PP^*}\right), \quad (\text{A12})$$

$$K_{1(2^-)} = \text{diag}\left(-\frac{1}{2\tilde{m}_{PP^*}} \Delta_1, -\frac{1}{2\tilde{m}_{PP^*}} \Delta_3, -\frac{1}{2\tilde{m}_{P^*P^*}} \Delta_1 + \Delta m_{PP^*}, -\frac{1}{2\tilde{m}_{P^*P^*}} \Delta_3 + \Delta m_{PP^*}\right), \quad (\text{A13})$$

where $\Delta_l = \frac{\partial^2}{\partial r^2} + \frac{2}{r} \frac{\partial}{\partial r} - \frac{l(l+1)}{r^2}$ with integer $l \geq 0$, $1/\tilde{m}_{PP} = 1/m_P + 1/m_P$, $1/\tilde{m}_{PP^*} = 1/m_P + 1/m_{P^*}$, $1/\tilde{m}_{P^*P^*} = 1/m_{P^*} + 1/m_{P^*}$.

The π exchange potentials for each $I(J^P)$ states are

$$V_{0(0^-)}^\pi = (V_C^\pi + 2V_T^\pi), \quad (\text{A14})$$

$$V_{0(1^+)}^\pi = \begin{pmatrix} -V_C^\pi & \sqrt{2}V_T^\pi & 2V_C^\pi & \sqrt{2}V_T^\pi \\ \sqrt{2}V_T^\pi & -V_C^\pi - V_T^\pi & \sqrt{2}V_T^\pi & 2V_C^\pi - V_T^\pi \\ 2V_C^\pi & \sqrt{2}V_T^\pi & -V_C^\pi & \sqrt{2}V_T^\pi \\ \sqrt{2}V_T^\pi & 2V_C^\pi - V_T^\pi & \sqrt{2}V_T^\pi & -V_C^\pi - V_T^\pi \end{pmatrix}, \quad (\text{A15})$$

$$V_{0(1^-)}^\pi = \begin{pmatrix} 0 & 0 & -\sqrt{3}V_C^\pi & -2\sqrt{\frac{3}{5}}V_T^\pi & 3\sqrt{\frac{2}{5}}V_T^\pi \\ 0 & V_C^\pi - V_T^\pi & 0 & -3\sqrt{\frac{3}{5}}V_T^\pi & -3\sqrt{\frac{2}{5}}V_T^\pi \\ -\sqrt{3}V_C^\pi & 0 & -2V_C^\pi & \frac{2}{\sqrt{5}}V_T^\pi & -\sqrt{\frac{6}{5}}V_T^\pi \\ -2\sqrt{\frac{3}{5}}V_T^\pi & -3\sqrt{\frac{3}{5}}V_T^\pi & \frac{2}{\sqrt{5}}V_T^\pi & V_C^\pi - \frac{7}{5}V_T^\pi & \frac{\sqrt{6}}{5}V_T^\pi \\ 3\sqrt{\frac{2}{5}}V_T^\pi & -3\sqrt{\frac{2}{5}}V_T^\pi & -\sqrt{\frac{6}{5}}V_T^\pi & \frac{\sqrt{6}}{5}V_T^\pi & V_C^\pi - \frac{8}{5}V_T^\pi \end{pmatrix}, \quad (\text{A16})$$

$$V_{0(2^+)}^\pi = \begin{pmatrix} -V_C^\pi + V_T^\pi & 2V_C^\pi + V_T^\pi \\ 2V_C^\pi + V_T^\pi & -V_C^\pi + V_T^\pi \end{pmatrix}, \quad (\text{A17})$$

$$V_{0(2^-)}^\pi = \begin{pmatrix} V_C^\pi + \frac{1}{5}V_T^\pi & -\frac{3\sqrt{6}}{5}V_T^\pi & \frac{3\sqrt{3}}{5}V_T^\pi & -\frac{6\sqrt{3}}{5}V_T^\pi \\ -\frac{3\sqrt{6}}{5}V_T^\pi & V_C^\pi + \frac{4}{5}V_T^\pi & \frac{3\sqrt{2}}{5}V_T^\pi & -\frac{6\sqrt{2}}{5}V_T^\pi \\ \frac{3\sqrt{3}}{5}V_T^\pi & \frac{3\sqrt{2}}{5}V_T^\pi & V_C^\pi + \frac{7}{5}V_T^\pi & \frac{6}{5}V_T^\pi \\ -\frac{6\sqrt{3}}{5}V_T^\pi & -\frac{6\sqrt{2}}{5}V_T^\pi & \frac{6}{5}V_T^\pi & V_C^\pi - \frac{2}{5}V_T^\pi \end{pmatrix}, \quad (\text{A18})$$

$$V_{1(0^+)}^\pi = \begin{pmatrix} 0 & -\sqrt{3}V_C^\pi & \sqrt{6}V_T^\pi \\ -\sqrt{3}V_C^\pi & -2V_C^\pi & -\sqrt{2}V_T^\pi \\ \sqrt{6}V_T^\pi & -\sqrt{2}V_T^\pi & V_C^\pi - 2V_T^\pi \end{pmatrix}, \quad (\text{A19})$$

$$V_{1(0^-)}^\pi = \begin{pmatrix} -V_C^\pi - 2V_T^\pi & 2V_C^\pi - 2V_T^\pi \\ 2V_C^\pi - 2V_T^\pi & -V_C^\pi - 2V_T^\pi \end{pmatrix}, \quad (\text{A20})$$

$$V_{1(1^+)}^\pi = \begin{pmatrix} V_C^\pi & -\sqrt{2}V_T^\pi & -\sqrt{6}V_T^\pi \\ -\sqrt{2}V_T^\pi & V_C^\pi + V_T^\pi & -\sqrt{3}V_T^\pi \\ -\sqrt{6}V_T^\pi & -\sqrt{3}V_T^\pi & V_C^\pi - V_T^\pi \end{pmatrix}, \quad (\text{A21})$$

$$V_{1(1^-)}^\pi = \begin{pmatrix} -V_C^\pi + V_T^\pi & -2V_C^\pi - V_T^\pi \\ -2V_C^\pi - V_T^\pi & -V_C^\pi + V_T^\pi \end{pmatrix}, \quad (\text{A22})$$

$$V_{1(2^+)}^\pi = \begin{pmatrix} 0 & 0 & -\sqrt{3}V_C^\pi & \sqrt{\frac{6}{5}}V_T^\pi & -2\sqrt{\frac{3}{7}}V_T^\pi & 6\sqrt{\frac{3}{35}}V_T^\pi \\ 0 & V_C^\pi - V_T^\pi & 0 & 3\sqrt{\frac{2}{5}}V_T^\pi & -\frac{3}{\sqrt{7}}V_T^\pi & -\frac{12}{\sqrt{35}}V_T^\pi \\ -\sqrt{3}V_C^\pi & 0 & -2V_C^\pi & -\sqrt{\frac{2}{5}}V_T^\pi & \frac{2}{\sqrt{7}}V_T^\pi & -\frac{6}{\sqrt{35}}V_T^\pi \\ \sqrt{\frac{6}{5}}V_T^\pi & 3\sqrt{\frac{3}{5}}V_T^\pi & -\sqrt{\frac{2}{5}}V_T^\pi & V_C^\pi & \sqrt{\frac{14}{5}}V_T^\pi & 0 \\ -2\sqrt{\frac{3}{7}}V_T^\pi & -\frac{3}{\sqrt{7}}V_T^\pi & \frac{2}{\sqrt{7}}V_T^\pi & \sqrt{\frac{14}{5}}V_T^\pi & V_C^\pi + \frac{3}{7}V_T^\pi & \frac{12}{7\sqrt{5}}V_T^\pi \\ 6\sqrt{\frac{3}{35}}V_T^\pi & -\frac{12}{\sqrt{35}}V_T^\pi & -\frac{6}{\sqrt{35}}V_T^\pi & 0 & \frac{12}{7\sqrt{5}}V_T^\pi & V_C^\pi - \frac{10}{7}V_T^\pi \end{pmatrix}, \quad (\text{A23})$$

$$V_{1(2^-)}^\pi = \begin{pmatrix} -V_C^\pi - \frac{1}{5}V_T^\pi & \frac{3\sqrt{6}}{5}V_T^\pi & 2V_C^\pi - \frac{1}{5}V_T^\pi & \frac{3\sqrt{6}}{5}V_T^\pi \\ \frac{3\sqrt{6}}{5}V_T^\pi & -V_C^\pi - \frac{4}{5}V_T^\pi & \frac{3\sqrt{6}}{5}V_T^\pi & 2V_C^\pi - \frac{4}{5}V_T^\pi \\ 2V_C^\pi - \frac{1}{5}V_T^\pi & \frac{3\sqrt{6}}{5}V_T^\pi & -V_C^\pi - \frac{1}{5}V_T^\pi & \frac{3\sqrt{6}}{5}V_T^\pi \\ \frac{3\sqrt{6}}{5}V_T^\pi & 2V_C^\pi - \frac{4}{5}V_T^\pi & \frac{3\sqrt{6}}{5}V_T^\pi & -V_C^\pi - \frac{4}{5}V_T^\pi \end{pmatrix}. \quad (\text{A24})$$

The ρ and ω potentials are

$$V_{0(0^-)}^v = (2V_C^v - 2V_T^v + V_C^{v'}), \quad (\text{A25})$$

$$V_{0(1^+)}^v = \begin{pmatrix} -2V_C^v + V_C^{v'} & -\sqrt{2}V_T^v & 4V_C^v & -\sqrt{2}V_T^v \\ -\sqrt{2}V_T^v & -2V_C^v + V_T^v + V_C^{v'} & -\sqrt{2}V_T^v & 4V_C^v + V_T^v \\ 4V_C^v & -\sqrt{2}V_T^v & -2V_C^v + V_C^{v'} & -\sqrt{2}V_T^v \\ -\sqrt{2}V_T^v & 4V_C^v + V_T^v & -\sqrt{2}V_T^v & -2V_C^v + V_T^v + V_C^{v'} \end{pmatrix}, \quad (\text{A26})$$

$$V_{0(1^-)}^v = \begin{pmatrix} V_C^{v'} & 0 & -2\sqrt{3}V_C^v & 2\sqrt{\frac{3}{5}}V_T^v & -3\sqrt{\frac{2}{5}}V_T^v \\ 0 & 2V_C^v + V_T^v + V_C^{v'} & 0 & 3\sqrt{\frac{3}{5}}V_T^v & -3\sqrt{\frac{2}{5}}V_T^v \\ -2\sqrt{3}V_C^v & 0 & -4V_C^v + V_C^{v'} & -\frac{2}{\sqrt{5}}V_T^v & \sqrt{\frac{6}{5}}V_T^v \\ 2\sqrt{\frac{3}{5}}V_T^v & 3\sqrt{\frac{3}{5}}V_T^v & -\frac{2}{\sqrt{5}}V_T^v & 2V_C^v + \frac{7}{5}V_T^v + V_C^{v'} & -\frac{\sqrt{6}}{5}V_T^v \\ -3\sqrt{\frac{2}{5}}V_T^v & -3\sqrt{\frac{2}{5}}V_T^v & \sqrt{\frac{6}{5}}V_T^v & -\frac{\sqrt{6}}{5}V_T^v & 2V_C^v + \frac{8}{5}V_T^v + V_C^{v'} \end{pmatrix}, \quad (\text{A27})$$

$$V_{0(2^+)}^v = \begin{pmatrix} -2V_C^v - V_T^v + V_C^{v'} & 4V_C^v - V_T^v \\ 4V_C^v - V_T^v & -2V_C^v - V_T^v + V_C^{v'} \end{pmatrix}, \quad (\text{A28})$$

$$V_{0(2^-)}^v = \begin{pmatrix} 2V_C^v - \frac{1}{5}V_T^v + V_C^{v'} & \frac{3\sqrt{6}}{5}V_T^v & -\frac{3\sqrt{3}}{5}V_T^v & \frac{6\sqrt{3}}{5}V_T^v \\ \frac{3\sqrt{6}}{5}V_T^v & 2V_C^v - \frac{4}{5}V_T^v + V_C^{v'} & -\frac{3\sqrt{2}}{5}V_T^v & \frac{6\sqrt{2}}{5}V_T^v \\ -\frac{3\sqrt{3}}{5}V_T^v & -\frac{3\sqrt{2}}{5}V_T^v & 2V_C^v - \frac{7}{5}V_T^v + V_C^{v'} & -\frac{6}{5}V_T^v \\ \frac{6\sqrt{3}}{5}V_T^v & \frac{6\sqrt{2}}{5}V_T^v & -\frac{6}{5}V_T^v & 2V_C^v + \frac{2}{5}V_T^v + V_C^{v'} \end{pmatrix}, \quad (\text{A29})$$

$$V_{1(0^+)}^v = \begin{pmatrix} V_C^{v'} & -2\sqrt{3}V_C^v & -\sqrt{6}V_T^v \\ -2\sqrt{3}V_C^v & -4V_C^v + V_C^{v'} & \sqrt{2}V_T^v \\ -\sqrt{6}V_T^v & \sqrt{2}V_T^v & 2V_C^v + 2V_T^v + V_C^{v'} \end{pmatrix}, \quad (\text{A30})$$

$$V_{1(0^-)}^v = \begin{pmatrix} -2V_C^v + 2V_T^v + V_C^{v'} & 4V_C^v + 2V_T^v \\ 4V_C^v + 2V_T^v & -2V_C^v + 2V_T^v + V_C^{v'} \end{pmatrix}, \quad (\text{A31})$$

$$V_{1(1^+)}^v = \begin{pmatrix} 2V_C^v + V_C^{v'} & \sqrt{2}V_T^v & \sqrt{6}V_T^v \\ \sqrt{2}V_T^v & 2V_C^v - V_T^v + V_C^{v'} & \sqrt{3}V_T^v \\ \sqrt{6}V_T^v & \sqrt{3}V_T^v & 2V_C^v + V_T^v + V_C^{v'} \end{pmatrix}, \quad (\text{A32})$$

$$V_{1(1^-)}^v = \begin{pmatrix} -2V_C^v - V_T^v + V_C^{v'} & -4V_C^v + V_T^v \\ -4V_C^v + V_T^v & -2V_C^v - V_T^v + V_C^{v'} \end{pmatrix}, \quad (\text{A33})$$

$$V_{1(2^+)}^v = \begin{pmatrix} V_C^{v'} & 0 & -2\sqrt{3}V_C^v & -\sqrt{\frac{6}{5}}V_T^v & 2\sqrt{\frac{3}{7}}V_T^v & -6\sqrt{\frac{3}{35}}V_T^v \\ 0 & 2V_C^v + V_T^v + V_C^{v'} & 0 & -3\sqrt{\frac{2}{5}}V_T^v & \frac{3}{\sqrt{7}}V_T^v & \frac{12}{\sqrt{35}}V_T^v \\ -2\sqrt{3}V_C^v & 0 & -4V_C^v + V_C^{v'} & \sqrt{\frac{2}{5}}V_T^v & -\frac{2}{\sqrt{7}}V_T^v & \frac{6}{\sqrt{35}}V_T^v \\ -\sqrt{\frac{6}{5}}V_T^v & 3\sqrt{\frac{3}{5}}V_T^v & \sqrt{\frac{2}{5}}V_T^v & 2V_C^v + V_C^{v'} & -\sqrt{\frac{14}{5}}V_T^v & 0 \\ 2\sqrt{\frac{3}{7}}V_T^v & \frac{3}{\sqrt{7}}V_T^v & -\frac{2}{\sqrt{7}}V_T^v & -\sqrt{\frac{14}{5}}V_T^v & 2V_C^v - \frac{3}{7}V_T^v + V_C^{v'} & -\frac{12}{7\sqrt{5}}V_T^v \\ -6\sqrt{\frac{3}{35}}V_T^v & \frac{12}{\sqrt{35}}V_T^v & \frac{6}{\sqrt{35}}V_T^v & 0 & -\frac{12}{7\sqrt{5}}V_T^v & 2V_C^v + \frac{10}{7}V_T^v + V_C^{v'} \end{pmatrix}, \quad (\text{A34})$$

$$V_{1(2^-)}^v = \begin{pmatrix} -2V_C^v + \frac{1}{5}V_T^v + V_C^{v'} & -\frac{3\sqrt{6}}{5}V_T^v & 4V_C^v + \frac{1}{5}V_T^v & -\frac{3\sqrt{6}}{5}V_T^v \\ -\frac{3\sqrt{6}}{5}V_T^v & -2V_C^v + \frac{4}{5}V_T^v + V_C^{v'} & -\frac{3\sqrt{6}}{5}V_T^v & 4V_C^v + \frac{4}{5}V_T^v \\ 4V_C^v + \frac{1}{5}V_T^v & -\frac{3\sqrt{6}}{5}V_T^v & -2V_C^v + \frac{1}{5}V_T^v + V_C^{v'} & -\frac{3\sqrt{6}}{5}V_T^v \\ -\frac{3\sqrt{6}}{5}V_T^v & 4V_C^v + \frac{4}{5}V_T^v & -\frac{3\sqrt{6}}{5}V_T^v & -2V_C^v + \frac{4}{5}V_T^v + V_C^{v'} \end{pmatrix}, \quad (\text{A35})$$

where the central and tensor potentials are defined as

$$V_C^\pi = \left(\sqrt{2}\frac{g}{f_\pi}\right)^2 \frac{1}{3} C(r; m_\pi) \vec{\tau}_1 \cdot \vec{\tau}_2, \quad (\text{A36})$$

$$V_T^\pi = \left(\sqrt{2}\frac{g}{f_\pi}\right)^2 \frac{1}{3} T(r; m_\pi) \vec{\tau}_1 \cdot \vec{\tau}_2, \quad (\text{A37})$$

$$V_C^\rho = (2\lambda g_V)^2 \frac{1}{3} C(r; m_\rho) \vec{\tau}_1 \cdot \vec{\tau}_2, \quad (\text{A38})$$

$$V_C^\omega = (2\lambda g_V)^2 \frac{1}{3} C(r; m_\omega), \quad (\text{A39})$$

$$V_T^\rho = (2\lambda g_V)^2 \frac{1}{3} T(r; m_\rho) \vec{\tau}_1 \cdot \vec{\tau}_2, \quad (\text{A40})$$

$$V_T^\omega = (2\lambda g_V)^2 \frac{1}{3} T(r; m_\omega), \quad (\text{A41})$$

$$V_C^{\rho'} = \left(\frac{\beta g_V}{2m_\rho}\right)^2 \frac{1}{3} C(r; m_\rho) \vec{\tau}_1 \cdot \vec{\tau}_2, \quad (\text{A42})$$

$$V_C^{\omega'} = \left(\frac{\beta g_V}{2m_\omega}\right)^2 \frac{1}{3} C(r; m_\omega). \quad (\text{A43})$$

-
- [1] N. Brambilla *et al.* (Quarkonium Working Group Collaboration), CERN Yellow Report No. CERN-2005-005, 2005.
[2] E. S. Swanson, *Phys. Rep.* **429**, 243 (2006).
[3] M. B. Voloshin, *Prog. Part. Nucl. Phys.* **61**, 455 (2008).

- [4] M. Nielsen, F. S. Navarra, and S. H. Lee, *Phys. Rep.* **497**, 41 (2010).
[5] N. Brambilla, *et al.*, *Eur. Phys. J. C* **71**, 1 (2011).
[6] S. Zouzou, B. Silvestre-Brac, C. Gignoux, and J. M. Richard, *Z. Phys. C* **30**, 457 (1986).
[7] H. J. Lipkin, *Phys. Lett. B* **172**, 242 (1986).

- [8] L. Heller and J. A. Tjon, *Phys. Rev. D* **35**, 969 (1987).
- [9] J. Carlson, L. Heller, and J. A. Tjon, *Phys. Rev. D* **37**, 744 (1988).
- [10] B. Silvestre-Brac and C. Semay, *Z. Phys. C* **57**, 273 (1993).
- [11] C. Semay and B. Silvestre-Brac, *Z. Phys. C* **61**, 271 (1994).
- [12] S. Pepin, F. Stancu, M. Genovese, and J. M. Richard, *Phys. Lett. B* **393**, 119 (1997).
- [13] D. M. Brink and F. Stancu, *Phys. Rev. D* **57**, 6778 (1998).
- [14] B. Silvestre-Brac and C. Semay, *Z. Phys. C* **59**, 457 (1993).
- [15] S. Pepin, F. Stancu, M. Genovese, and J. M. Richard, *Phys. Lett. B* **393**, 119 (1997).
- [16] J. Schaffner-Bielich and A. P. Vischer, *Phys. Rev. D* **57**, 4142 (1998).
- [17] D. Janc and M. Rosina, *Few-Body Syst.* **35**, 175 (2004).
- [18] N. Barnea, J. Vijande, and A. Valcarce, *Phys. Rev. D* **73**, 054004 (2006).
- [19] J. Vijande, E. Weissman, N. Barnea, and A. Valcarce, *Phys. Rev. D* **76**, 094022 (2007).
- [20] J. Vijande, E. Weissman, A. Valcarce, and N. Barnea, *Phys. Rev. D* **76**, 094027 (2007).
- [21] D. Ebert, R. N. Faustov, V. O. Galkin, and W. Lucha, *Phys. Rev. D* **76**, 114015 (2007).
- [22] F. S. Navarra, M. Nielsen, and S. H. Lee, *Phys. Lett. B* **649**, 166 (2007).
- [23] S. H. Lee, S. Yasui, W. Liu, and C. M. Ko, *Eur. Phys. J. C* **54**, 259 (2008).
- [24] S. H. Lee and S. Yasui, *Eur. Phys. J. C* **64**, 283 (2009).
- [25] M. Zhang, H. X. Zhang, and Z. Y. Zhang, *Commun. Theor. Phys.* **50**, 437 (2008).
- [26] Y. Yang, C. Deng, J. Ping, and T. Goldman, *Phys. Rev. D* **80**, 114023 (2009).
- [27] J. Vijande, A. Valcarce, and N. Barnea, *Phys. Rev. D* **79**, 074010 (2009).
- [28] T. F. Carames, A. Valcarce, and J. Vijande, *Phys. Lett. B* **699**, 291 (2011).
- [29] J. Vijande, A. Valcarce, and T. F. Carames, *Few-Body Syst.* **50**, 195 (2010).
- [30] J. P. Ader, J. M. Richard, and P. Taxil, *Phys. Rev. D* **25**, 2370 (1982).
- [31] J. Vijande, A. Valcarce, and J. M. Richard, *Phys. Rev. D* **76**, 114013 (2007).
- [32] A. V. Manohar and M. B. Wise, *Nucl. Phys.* **B399**, 17 (1993).
- [33] N. A. Tornqvist, *Z. Phys. C* **61**, 525 (1994).
- [34] G.-J. Ding, J.-F. Liu, and M.-L. Yan, *Phys. Rev. D* **79**, 054005 (2009).
- [35] R. Molina, T. Branz, and E. Oset, *Phys. Rev. D* **82**, 014010 (2010).
- [36] R. L. Jaffe, *Phys. Rev. D* **15**, 267 (1977).
- [37] R. L. Jaffe, *Phys. Rev. D* **17**, 1444 (1978).
- [38] R. L. Jaffe and F. Wilczek, *Phys. Rev. Lett.* **91**, 232003 (2003).
- [39] M. G. Alford, K. Rajagopal, and F. Wilczek, *Phys. Lett. B* **422**, 247 (1998).
- [40] R. Rapp, T. Schafer, E. V. Shuryak, and M. Velkovsky, *Phys. Rev. Lett.* **81**, 53 (1998).
- [41] M. G. Alford, A. Schmitt, K. Rajagopal, and T. Schafer, *Rev. Mod. Phys.* **80**, 1455 (2008).
- [42] Y. Nambu and G. Jona-Lasinio, *Phys. Rev.* **122**, 345 (1961); **124**, 246 (1961).
- [43] G. Burdman and J. F. Donoghue, *Phys. Lett. B* **280**, 287 (1992).
- [44] M. B. Wise, *Phys. Rev. D* **45**, R2188 (1992).
- [45] T. M. Yan, H. Y. Cheng, C. Y. Cheung, G. L. Lin, Y. C. Lin, and H. L. Yu, *Phys. Rev. D* **46**, 1148 (1992); T. M. Yan, H. Y. Cheng, C. Y. Cheung, G. L. Lin, Y. C. Lin, H. L. Yu, *ibid.* **55**, 5851(E) (1997).
- [46] R. Casalbuoni, A. Deandrea, N. Di Bartolomeo, R. Gatto, F. Feruglio, and G. Nardulli, *Phys. Rep.* **281**, 145 (1997).
- [47] A. V. Manohar and M. B. Wise, *Cambridge Monogr. Part. Phys., Nucl. Phys., Cosmol.* **10**, 1 (2000).
- [48] C. Isola, M. Ladisa, G. Nardulli, and P. Santorelli, *Phys. Rev. D* **68**, 114001 (2003).
- [49] S. Ohkoda, Y. Yamaguchi, S. Yasui, K. Sudoh, and A. Hosaka, *Phys. Rev. D* **86**, 014004 (2012).
- [50] S. Yasui and K. Sudoh, *Phys. Rev. D* **80**, 034008 (2009).
- [51] Y. Yamaguchi, S. Ohkoda, S. Yasui, and A. Hosaka, *Phys. Rev. D* **84**, 014032 (2011).
- [52] Y. Yamaguchi, S. Ohkoda, S. Yasui, and A. Hosaka, *Phys. Rev. D* **85**, 054003 (2012).
- [53] B. R. Johnson, *J. Chem. Phys.* **69**, 10 (1978).
- [54] K. Arai and A. T. Kruppa, *Phys. Rev. C* **60**, 064315 (1999).
- [55] S. Aoyama, T. Myo, K. Kato, and K. Ikeda, *Prog. Theor. Phys.* **116**, 1 (2006).
- [56] A. D. Fabbro, D. Janc, M. Rosina, and D. Treleani, *Phys. Rev. D* **71**, 014008 (2005).
- [57] S. Cho *et al.* (ExHIC Collaboration), *Phys. Rev. Lett.* **106**, 212001 (2011).
- [58] S. Cho *et al.* (ExHIC Collaboration), *Phys. Rev. C* **84**, 064910 (2011).